Hindawi
Shock and Vibration
Volume 2020, Article ID 6021640, 12 pages
https://doi.org/10.1155/2020/6021640

Research Article

A Method of Reducing Motor Vibration: Natural Frequency, Damping Ratio, and Vibration Analysis of CFRP Motor Frame

Jinguang Zhang[1,2], **Hairu Yang**[1,3], **Xiong Li**[1] and **Wei Ye**[1,2]

[1]*School of Mechanical and Electronic Engineering, Wuhan University of Technology, Luoshi Road 122, Wuhan 430070, Hubei, China*
[2]*Institute of Advanced Material Manufacturing Equipment and Technology, Wuhan University of Technology, Luoshi Road 122, Wuhan 430070, Hubei, China*
[3]*School of Electromechanical and Automobile Engineering, Huanggang Normal University, Xinganger Road 146, Huanggang 438000, Hubei, China*

Correspondence should be addressed to Hairu Yang; yhrcgz@126.com

Received 19 September 2019; Revised 24 November 2019; Accepted 16 December 2019; Published 11 January 2020

Guest Editor: Said Elias

The existing motor frame is made of metal materials. In this paper, a carbon fiber reinforced plastic (CFRP) motor frame, which uses material damping to reduce vibration amplitude, which is proposed to design and manufacture low-vibration motors. The damp ratio of the CFRP motor frame is calculated by the damp prediction model based on strain energy, which is verified by the combination of the finite element method and experiment. The vibration characteristics of the CFRP frame motor are studied experimentally and compared with that of the metal frame motor. The results show that the CFRP frame motor has good vibration reduction. The amplitude reduction is up to 5 times higher than that of the metal motor frame, which proves that the damping vibration reduction of the CFRP motor frame has a good application value.

1. Introduction

The motor is widely used for power source. The vibration reduction motor has important application value for reducing the vibration of the equipment system. Motor vibration involves many disciplines and fields. Some scholars have studied the vibration characteristics of the motor structure. Mendon et al. [1] has studied the dynamic characteristics of the composite rotor. It is found that different laminate composite can obtain a rotor with different critical speed of rotation, instability threshold, and frequency response characteristics. Druesne et al. [2] used the structural dynamic finite element coupling model to analyze the dynamic characteristics of the motor stator under electromagnetic vibration and mechanical vibration. It is found that Young's modulus and density of stator material have a great influence on the natural frequency and vibration response signal.

At present, most motor frames are made of cast iron, aluminum alloy, and other metal materials, but the damping of metal materials is limited, which cannot play a very good vibration. Carbon fiber reinforced composites (CFRP) are a new type of structural and functional composite material with high specific modulus, high specific strength, light weight, and high strength. It also has excellent damping performance and can be directly used in the structure with vibration amplitude reduction [3–5]. Adams and Bacon [6] and Ni and Adams [7] believe that the damping contribution of composite material comes from the stress components inside the material and each direction has different loss factors. The damping of composite material can be defined as the ratio of the sum of energy dissipation of strain in all directions to the total strain energy in one vibration cycle. Billups and Cavalli [8] used the modal strain energy model to study the damping performance of the composite thin plate structure with alternate sequential layup. With the increase

of the layup angle, the specific damping capacity of the structure is increased, reaching a maximum of 10% at 35°. Martone et al. [9] and Assarar et al. [10] studied the damping properties of composites plate and cantilever beam structures; Abramovich et al. [11] studied the damping characteristics of composites laminates for aerocraft structural components in depth. Composites laminates have larger damping loss factors. Maheri [12] summarized the influencing factors affecting the damping properties of fiber reinforced composites and found that the damping ratio of a woven fabric layer is about 4 times that of the unidirectional fabric layer; Rueppel et al. [13] used the logarithmic decay method, DMA analysis, and vibration beam method to study the damping performance of the CFRP laminate structure. The results show that the damping of composite structure increases with the angle of the laminate when the frequency is below 300 Hz. Hong et al. [14] proposed a hybrid method to predict the structural damping of the composite blade. Zhang et al. [15] have studied on CFRP and metal raft frame, and the results show that the CFRP raft frame has good vibration isolation performance. Wen et al. [16] studied the vibration characteristics of the CFRP truss raft. In summary, the study of vibration damping properties of composite materials is a frontier in the field of composite material science.

In the paper, starting from the improvement of the damping of the material of the motor frame, a three-phase asynchronous motor of a certain type, the structure design of the CFRP motor frame is carried out based on the excellent damping performance and establishes a damping prediction model based on the strain energy loss. Finally, the modal experiment and vibration test of the CFRP frame motor are carried out and compared with the vibration of the metal frame motor, and the vibration effect of the frame damping is proved, which has an important application value for reducing the vibration amplitude of the equipment system.

2. Design of CFRP Motor Frame Structure

In this paper, the JW6314 three-phase asynchronous motor is selected as the reference. According to the aluminum alloy frame (nonmagnetic machine frame) of this type of motor, the structure of the CFRP motor frame is designed. Table 1 shows the performance parameters of the JW6314 three-phase motor. Figure 1 is a structural of the JW6314 motor frame, which is casted by aluminum alloy. The motor is driven with constant magnetization at each speed. The stator core, winding, rotor, rotating shaft, end cover, and other components used in the assembly of CFRP motors are all original parts of JW6314. Considering the difficulty and economy of molding, the structural of the CFRP motor frame is changed. In order to facilitate manufacture, the CFRP motor frame is divided into three parts: cylinder, base, and metal connecting ring, as shown in Figure 2, wherein the cylinder and the base are molded by a carbon fiber composite prep-reg and fixed together by gluing. The material used for the metal connecting ring is 45 steel, which is fixed together with the cylindrical by gluing and short pin.

Table 1: JW6314 motor parameters.

Voltage	380 V	Insulation grade	B
Current	0.65 A	Protection level	IP44
Power	0.18 KW	Cooling mode	IC411
Rotation rate	1440 r/min	Working days	S1
Number of poles	4	Rated frequency	50 Hz

Figure 1: Aluminum alloy frame of the JW6314 motor.

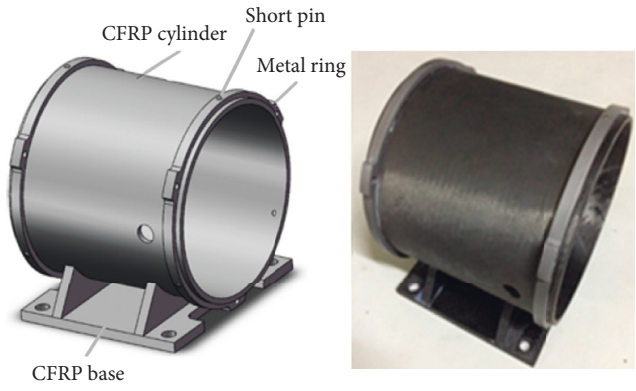

Figure 2: CFRP motor frame.

3. Numerical Analysis of Natural Frequency and Damping Ratio of the CFRP Motor Frame

Natural frequency and damping are the main parameters that affect the vibration of the equipment. The finite element model of the CFRP motor frame shown in Figure 3 is built in the Abaqus finite element simulation software, which is measured in a free-free condition. The CFRP motor frame is made of pre-preg of type T700/YPH-42T. The lamination of the cylinder is $[45^\circ/-45^\circ/45^\circ]_{5S}$, and the lamination of the motor base is $[0^\circ/90^\circ]_{15S}$. The sweeping method is used to divide the hexahedral finite element meshes. The linear reduced integral element C3D8R is chosen. The number of elements in the cylinder part is 5808, in the base part is 4142, and in the metal connecting ring is 1456. The modal analysis of the CFRP motor and the aluminum alloy frame are

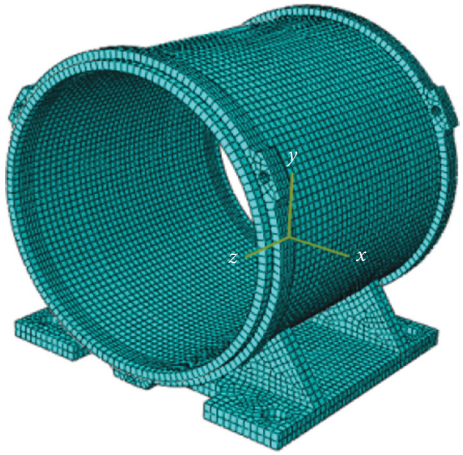

Figure 3: Finite element model of the CFRP Motor frame.

carried out, respectively. The frequency analysis step linear perturbation is set. The first 3 modes are analyzed.

3.1. Study on Natural Frequency and Mode Shapes of the Motor Frame. The modal analysis of the CFRP and the aluminum alloy motor frame are carried out, respectively, and the first 3 modal frequencies of the motor frame are obtained, as shown in Table 2. The natural frequency of each mode of the CFRP motor frame is higher than that of the metal frame, and the first modal frequency is about 9 times of that of the metal frame. Because the specific strength and specific rigidity of CFRP are higher than that of aluminum alloy and the density of CFRP is lower than that of aluminum alloy, the natural frequency characteristics of the CFRP motor frame are obviously better than that of the metal frame when the size is the same. The rated speed of JW6314 is 1440 r/min, converted into frequency is 24 Hz, which is far less than the first-mode frequency of the CFRP motor frame. Therefore, when only considering the rotating vibration of the motor, the CFRP motor frame can effectively avoid the resonance.

The first three-mode shapes of the motor frame are shown in Figure 4. The 3 mode shapes of the two types of motor frames are consistent. The deformation of the cylinder is larger, and the base part is smaller. This is mainly because the cylinder part is a thin-walled, and the rigidity is smaller than the base. If you want to enhance the stiffness of the motor frame, the stiffness of the cylinder can be improved.

3.2. Damping of the CFRP Motor Frame. In order to capture the damping ratios of the CFRP motor frame, firstly, the stress-strain of each mode should be obtained. With the Abaqus finite element simulation software, the frequency and mode shapes of the CFRP motor frame in free mode are extracted by the Lanczos method and the strain information of each element is derived in postprocessing. Figure 5 shows the strain components in six directions in the first mode of the CFRP motor frame. Then, a program is written in MATLAB to calculate the loss factor of the structure. The flow chart of the calculation is shown in Figure 6.

Table 2: The first 3 modal frequencies of the motor frame/Hz.

	First mode	Second mode	Third mode
CFRP motor frame	535	710	943
JW6314 metal motor frame	60	143	163

Input the elements number of the cylinder part $N_1 = 5808$, the base part is $N_2 = 4142$, and the layers are $n = 30$. The stress and strain information of each layer elements can be derived in postprocessing. The strain energy dissipation and strain energy is calculated, according to formulas (2) and (3). The damping ratio of the structure is obtained, according to formulas (1) and (5).

Because the CFRP motor frame includes carbon fiber composite and metal connection ring, there are two parts of strain energy dissipation. According to Adams and Bacon's model [17], the loss factor of the CFRP motor frame is as follows:

$$\eta = \frac{\eta_m U_m + \Delta U_c}{U_m + U_c}. \tag{1}$$

In the above formula, η_m is the damping loss factor of the metal material, U_m is the maximum strain energy of the metal material part, U_c is the maximum strain energy of the carbon fiber composite part, and ΔU_c is the strain energy loss.

According to the Adams-Bacon damping strain energy model, the strain energy loss and the total strain energy of the structure can be expressed as follows:

$$\Delta U = \sum_{k=1}^{n}\sum_{i=1}^{3}\sum_{j=1}^{3}\eta_{ij}U_{ij}^{k} = \sum_{k=1}^{n}\sum_{i=1}^{3}\sum_{j=1}^{3}\frac{1}{2}\int \eta_{ij}\sigma_{ij}^{k}\varepsilon_{ij}^{k}dV^{k}, \tag{2}$$

$$U = \sum_{k=1}^{n}\sum_{i=1}^{3}\sum_{j=1}^{3}U_{ij}^{k} = \sum_{k=1}^{n}\sum_{i=1}^{3}\sum_{j=1}^{3}\frac{1}{2}\int \sigma_{ij}^{k}\varepsilon_{ij}^{k}dV^{k}. \tag{3}$$

In the above formula, V^k shows the unit integral volume in the kth layer of the laminated structure and σ_{ij}^{k}, $\varepsilon_{ij}^{k}(i, j = 1, 2, 3)$ represents the stress and strain components in the six directions of the kth layer of the laminated structure, among which direction 1 shows the fiber direction, directions 2 and 3 indicate the transverse direction. $\eta_{ij}^{k}(i, j = 1, 2, 3)$ shows the damping loss factors of anisotropic materials in six directions of the CFRP. The damping loss factor of the T700/YPH-42T material used in the CFRP motor frame is $\eta_{11} = 0.82\%$, $\eta_{22} = 2.98\%$, and $\eta_{12} = 8.57\%$ [18]. Since the 2–3 plane of CFRP is isotropic, the damping loss factor in the shear direction of the material is considered to be equal; therefore, there is $\eta_{22} = \eta_{33}$ and $\eta_{12} = \eta_{13} = \eta_{23}$.

After obtaining the first-mode loss factor (η) of the CFRP motor frame, the damping ratios (ξ) of other modes can be captured according to formulas (4) and (5). Similarly, other second-mode strain components can be derived from Abaqus and the damping ratio results of the CFRP motor frame are shown in Table 3.

In this paper, the material used for the metal connection ring of the CFRP motor frame is 45 steel, and the damping loss factor is 0.03%.

Modal mode	Mode shape of CFRP motor frame	Mode shape of JW6314 metal motor frame
The first mode shape	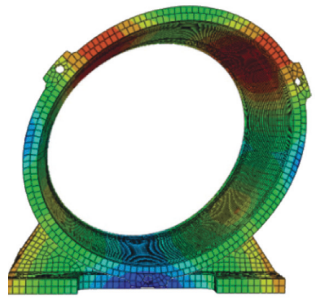	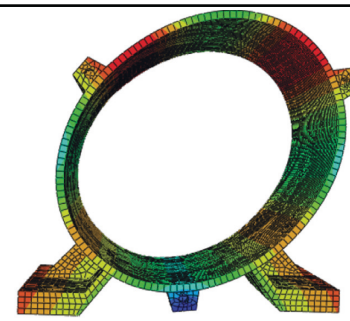
The second mode shape	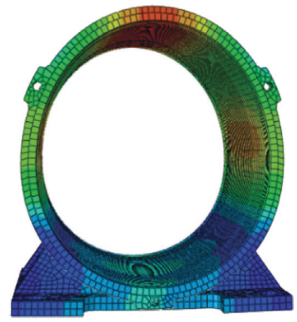	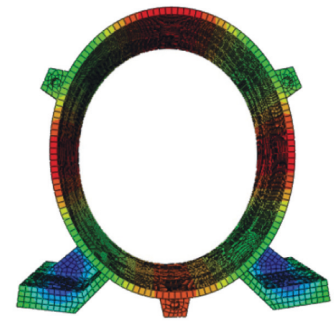
The third mode shape	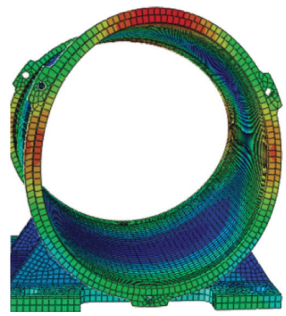	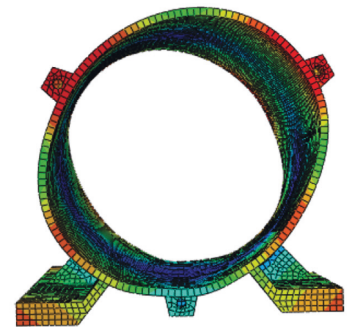

Figure 4: The first three-mode shapes of the CFRP and metal motor frame.

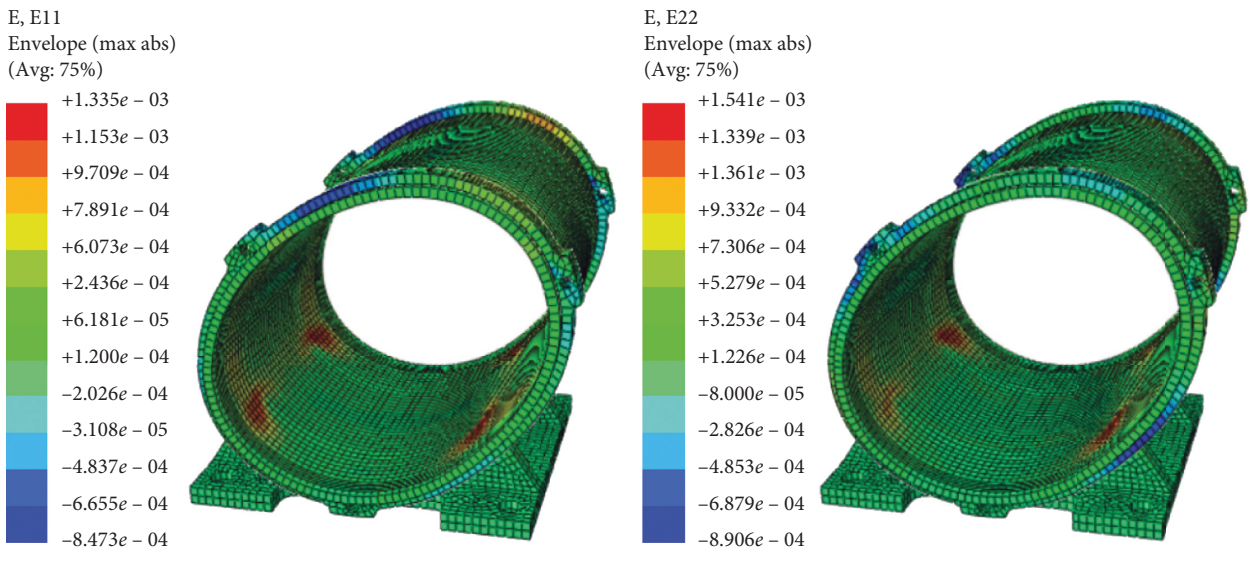

(a) (b)

Figure 5: Continued.

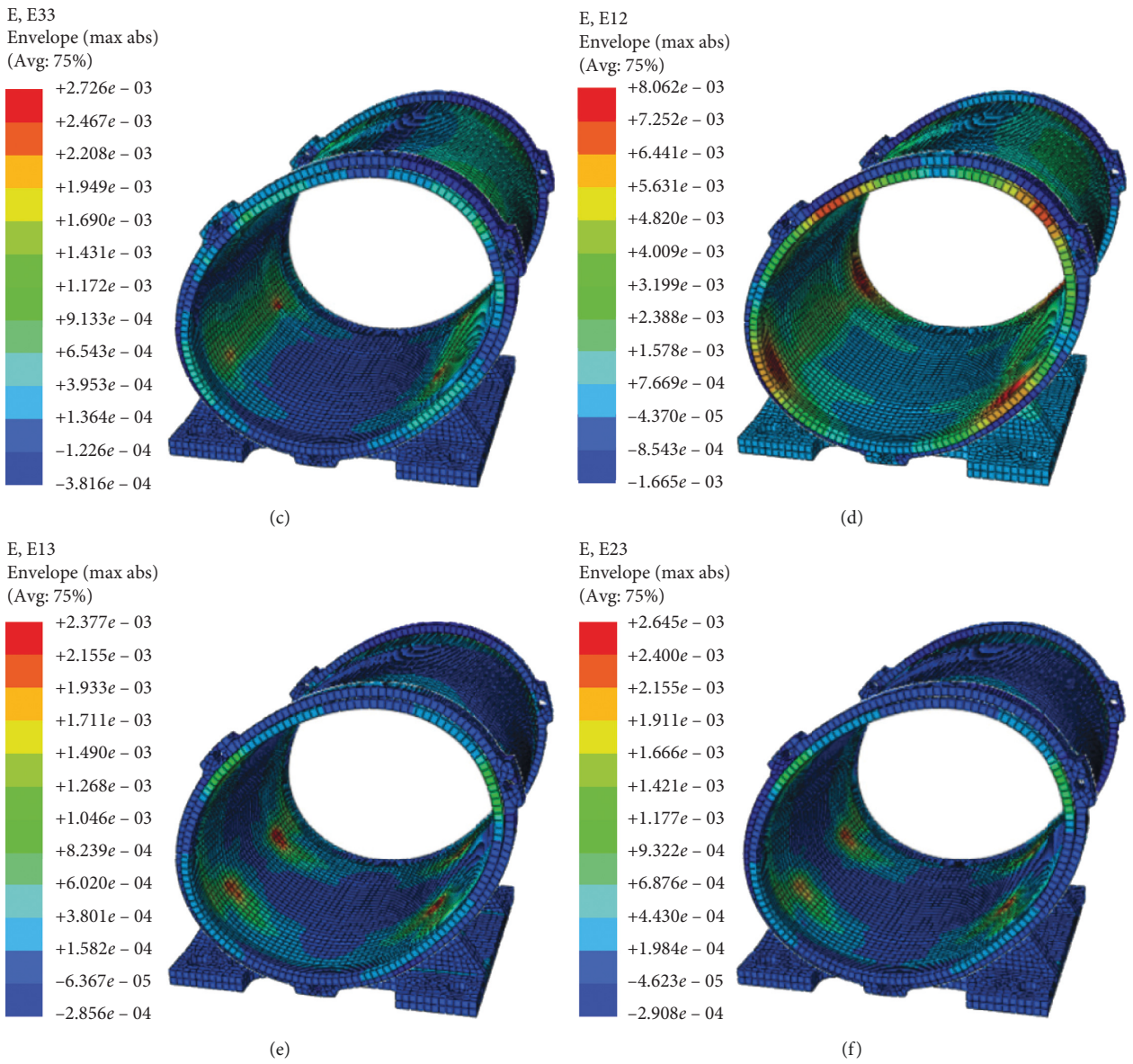

Figure 5: Strain components of the CFRP motor frame in all directions in the first mode. (a) 11-directional strain component, (b) 22-directional strain component, (c) 33-directional strain component, (d) 12-directional strain component, (e) 13-directional strain component, and (f) 23-directional strain component.

$$\eta = \frac{\psi}{2\pi}, \tag{4}$$

$$\xi = \frac{\eta}{\sqrt{4+\eta^2}}, \tag{5}$$

where Ψ is damping ratio capacity.

4. Experimental Study on Vibration of the CFRP Motor Frame

4.1. Modal Experiment of the CFRP Motor Frame. Modal experiment of the CFRP motor frame use the BK vibration testing equipment, hang the frame with elastic cord, and attach two voltage accelerometers sensor with sensitivity of 102.98 mv/g and 105.60 mv/g to the surface of the frame, as shown in Figure 7. Frequency response data obtained from modal experiments are imported into Modal Genius (as shown in Figure 8). The frequency response function of the test system is solved by using the single reference operational mode analysis method. Red lines are fitting curve, and the highest point represents the resonance peak. The second and third mode modal frequency and damping ratio of the specimens are as shown in Figure 8.

From Figure 8, it can be seen that the frequency response signal is unstable in the range of 0–700 Hz, which make the peak value not concentrated. The first-mode frequency is

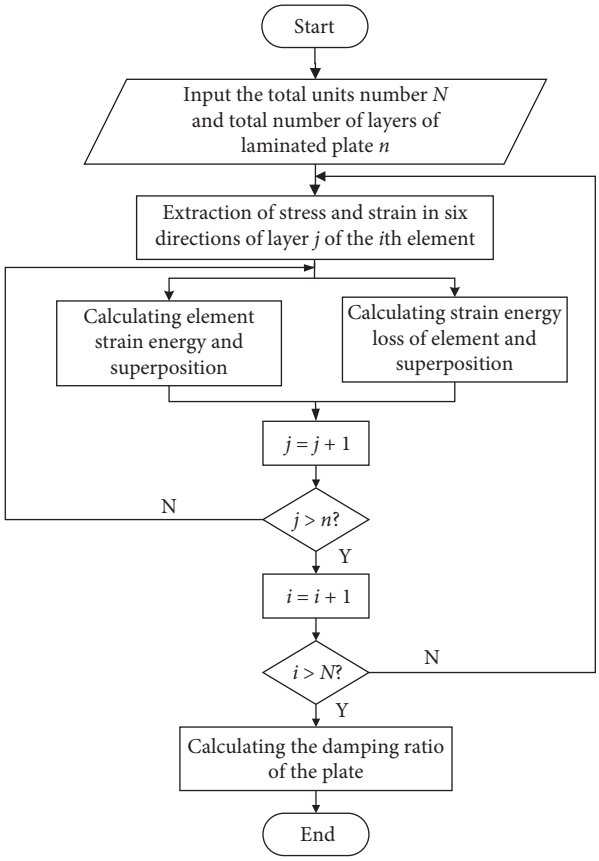

Figure 6: Flow chart of damping ratio calculation.

Table 3: Calculation of the damping ratio of the CFRP motor frame.

	First mode	Second mode	Third mode
Damping ratio ξ (%)	1.00	0.97	0.80

between 500-–600 Hz, and frequency and damping ratio can obtained from Modal Genius software. Compared the experimental value with the numerical calculation, and the results are shown in Table 4.

4.2. Characteristics Test of Motor Vibration. Vibration tests of two motors (as shown in Figure 9) are carried out. The vibration acceleration of two kinds of motors was measured. The stator core, winding, rotor, rotating shaft, end cover, and other components used in the assembly of CFRP motors are all original parts of JW6314. That is, except for the CFRP frame, other accessories are consistent with the JW6314 motor, and the assembling process is the same. The vibration source is the vibration caused by the unbalance rotor.

4.2.1. Vibration Test of the CFRP Frame Motor. Fix the motor to the foundation of the test bench by anchor bolts. The platform of the vibration test is shown in Figure 10. Acceleration sensors 2, 3, and 4 are, respectively, attached on the cylinder surface of the CFRP motor, and acceleration sensor 1 is attached on the base of the CFRP motor. Before the test, the four acceleration sensors are connected to the input channel of the conditioning amplifier, in order to obtain a steady and clear acceleration signal, the low-pass filter is connected to the output of the conditioning amplifier and the cut-off frequency is set to 73 Hz. Vibration signals from low-pass filters are transmitted to the data acquisition instrument in turn, and the acceleration signals are collected and analyzed by dynamic signal analysis software. The accelerometer arrangement is shown in Figure 11.

The sampling frequency is set to 146 Hz and the recording time is 3 s. Adjust the output of the frequency converter so that the speed of the CFRP motor is 1000 r/min, 1100 r/min, 1200 r/min, 1300 r/min, 1400 r/min, and 1500 r/min in sequence. After adjustment of the frequency converter, let the motor run for 1 min, then obtain the vibration acceleration of CFRP motor at different speeds. In order to accurately evaluate the vibration performance of the CFRP frame, the time-domain signals are transformed into fast Fourier transform. The vibration acceleration at each speed is analyzed in the frequency domain near the rotation frequency of the motor, that is, only the rotation vibration of the motor is considered. The results are shown in Figure 12.

It can be found from Figure 12(a) that only the rotational vibration amplitude of the rotor is considered, the vibration acceleration on the base increases as the motor speed increases, and the acceleration increases when the speed increases from 1000 r/min to 1500 r/min, with a growth of 94%; it can be seen from Figure 12(c) that the motor speed increases from 1000 r/min to 1500 r/min, the acceleration on the cylinder shell does not change much, and its increase is only 17%. The vibration acceleration of the cylinder shells in the horizontal direction (sensor 2 and 4 which are shown in Figures 12(b) and 12(d)) suddenly decreases to the minimum value at 1100 r/min and then changes little.

4.2.2. JW6314 Three-Phase Motor Vibration Test. As the test conditions of the CFRP frame motor, the analysis of the vibration acceleration in the JW6314 metal motor at different speeds is obtained. The results are shown in Figure 13.

It can be seen from Figure 13(a) that when only the rotational vibration of the motor rotor is considered, the vibration acceleration of the JW6314 three-phase motor frame increases with the rotational speed. When the rotational speed increases from 1000 r/min to 1500 r/min, the acceleration increase was 130%; there was no significant change on the cylinder of the JW6314 three-phase motor, as shown in Figure 13(c). The vibration acceleration of the cylinder shell in the horizontal direction, as shown in Figures 13(b) and 13(d), suddenly decreases to the minimum value at 1100 r/min and then changes little. From the Figures 13(b) and 13(d), it can be found that the JW6314 motor frame is disturbed seriously by the external environment.

5. Results Comparison Analysis

The vibration during the operation of the motor includes many reasons, such as the rotating vibration of the rotor, the

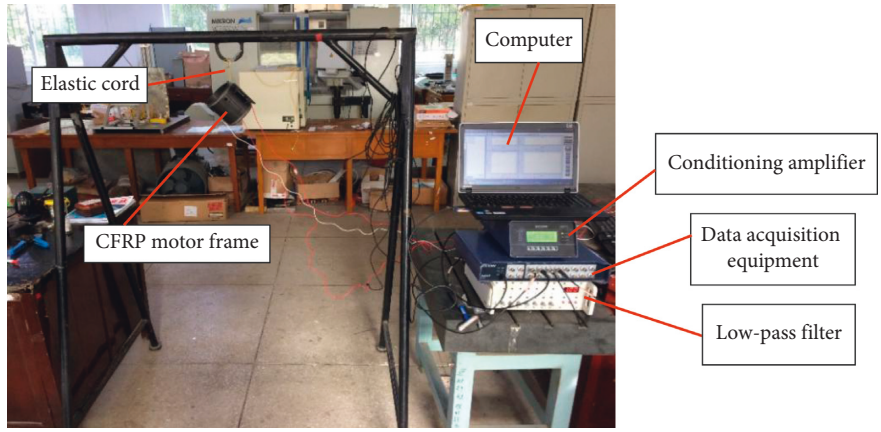

Figure 7: Modal experiment of the CFRP motor frame.

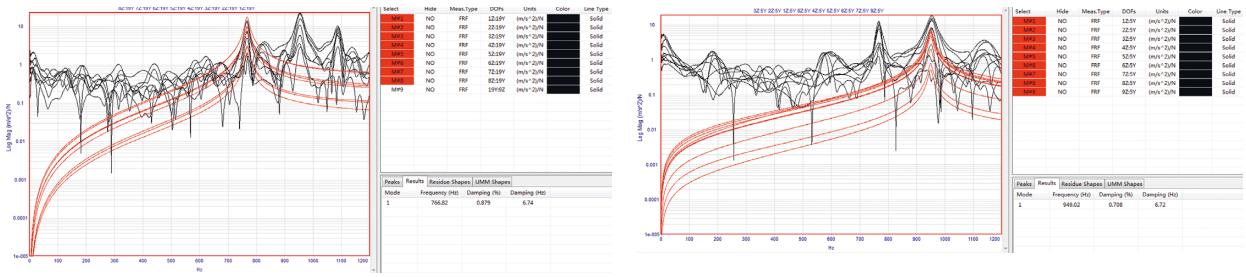

(a) (b)

Figure 8: Frequency and damping ratio of the CFRP motor frame. (a) Second-Mode Modal. (b) Third-Mode Modal.

Table 4: Modal Experimental results of the CFRP motor frame.

	Natural frequency			Damping ratio		
	Test (Hz)	FEA (Hz)	Error (%)	Test (%)	FEA (%)	Error (%)
First mode	559	530	5.5	0.91	1	9
Second mode	767	710	7.43	0.88	0.97	11.49
Third mode	950	943	0.73	0.69	0.80	15.94

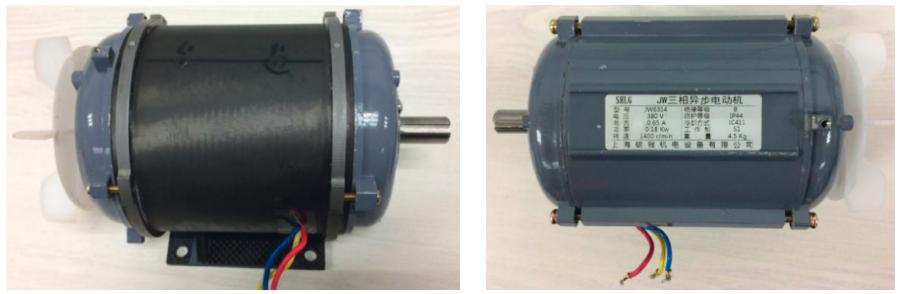

(a) (b)

Figure 9: (a) Motor of CFRP frame. (b) JW6314 three-phase Asynchronous Motor.

electromagnetic excitation between the stator and the rotor, and the vibration caused by the installation problems. In order to make a more accurate evaluation of the vibration reduction performance of the CFRP frame, the vibration acceleration of the two motors near the rotational frequency of the rotor is studied. The results are shown in Figure 14.

It can be seen from Figure 14 that the motor speed is between 1000 r/min and 1500 r/min. The vibration of the two motors near the rotating frequency shows that the vibration acceleration of the CFRP motor base and the cylinder shell is less than that of the JW6314 three-phase motor, that is to say, the CFRP motor frame shows good vibration amplitude

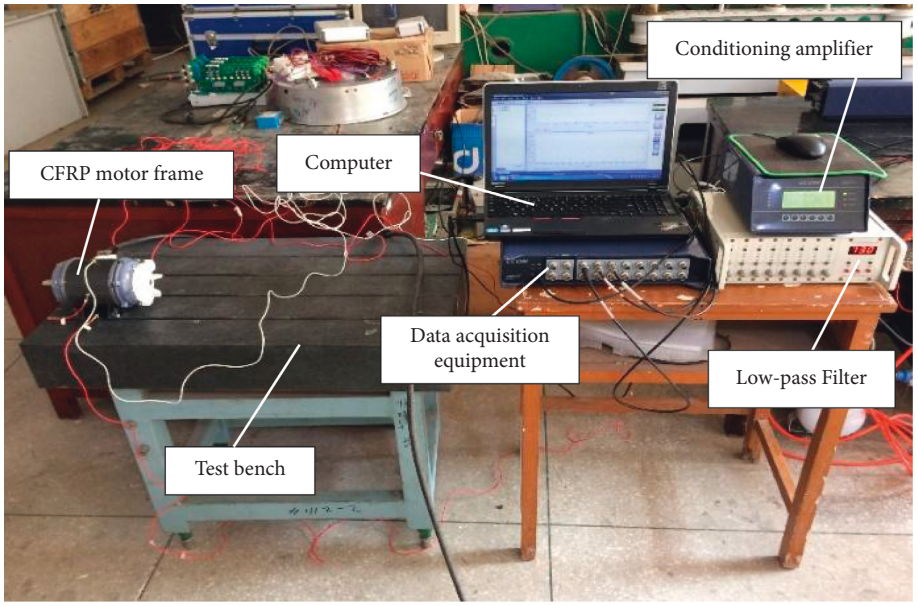

Figure 10: Vibration testing of the CFRP frame motor.

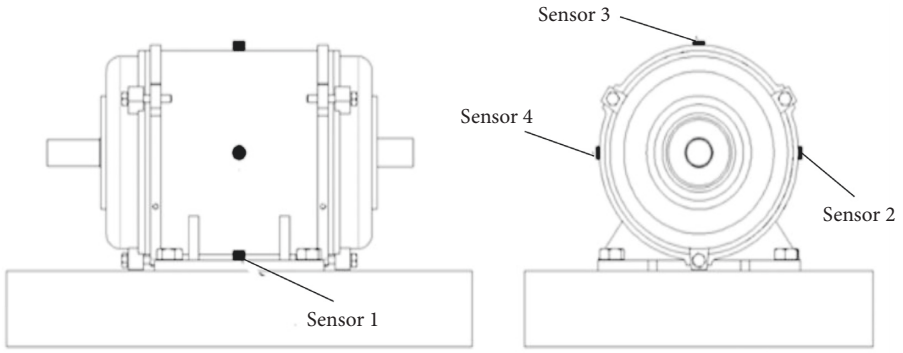

Figure 11: Arrangement of the acceleration sensor.

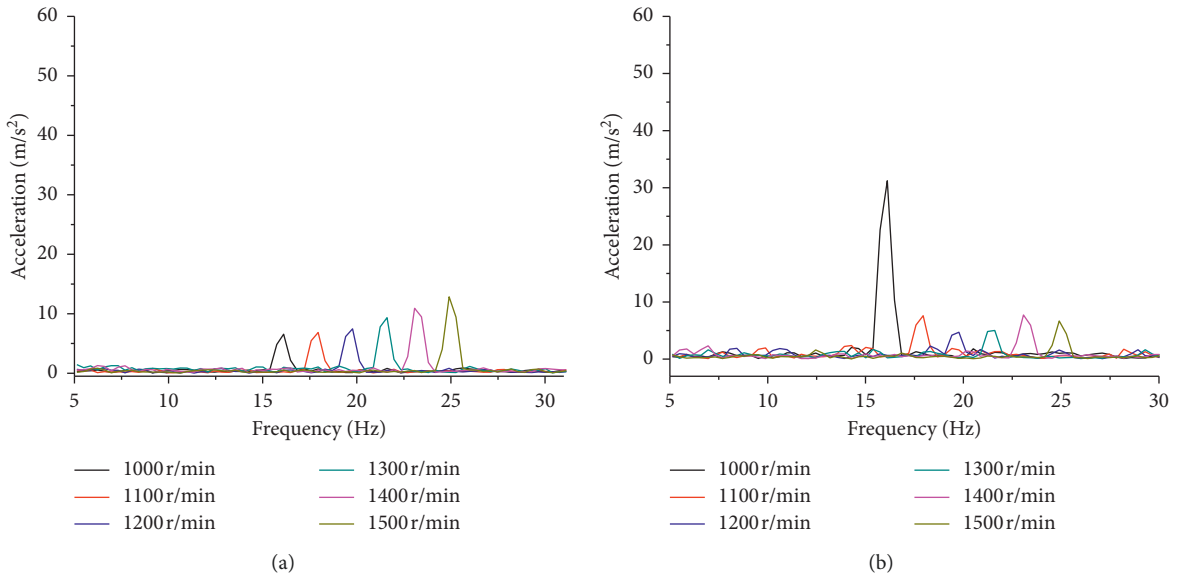

Figure 12: Continued.

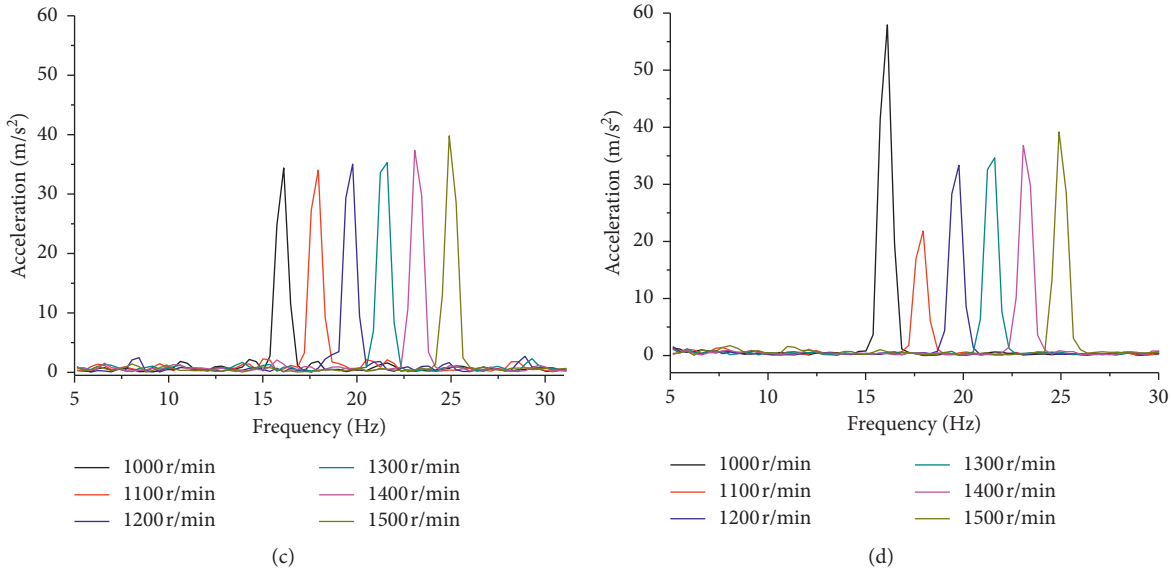

Figure 12: Vibration acceleration rotation frequency of the CFRP frame motor. (a) Sensor 1 on the base. (b) Sensor 2 on the cylinder shell. (c) Sensor 3 on the cylinder shell. (d) Sensor 4 on the cylinder shell.

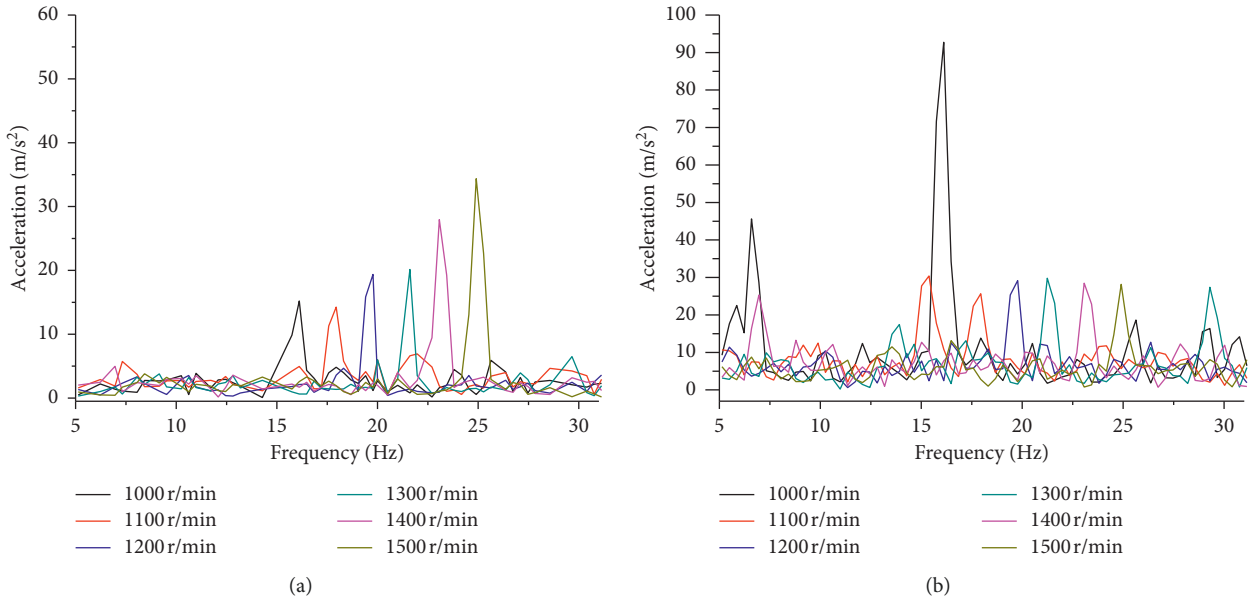

Figure 13: Continued.

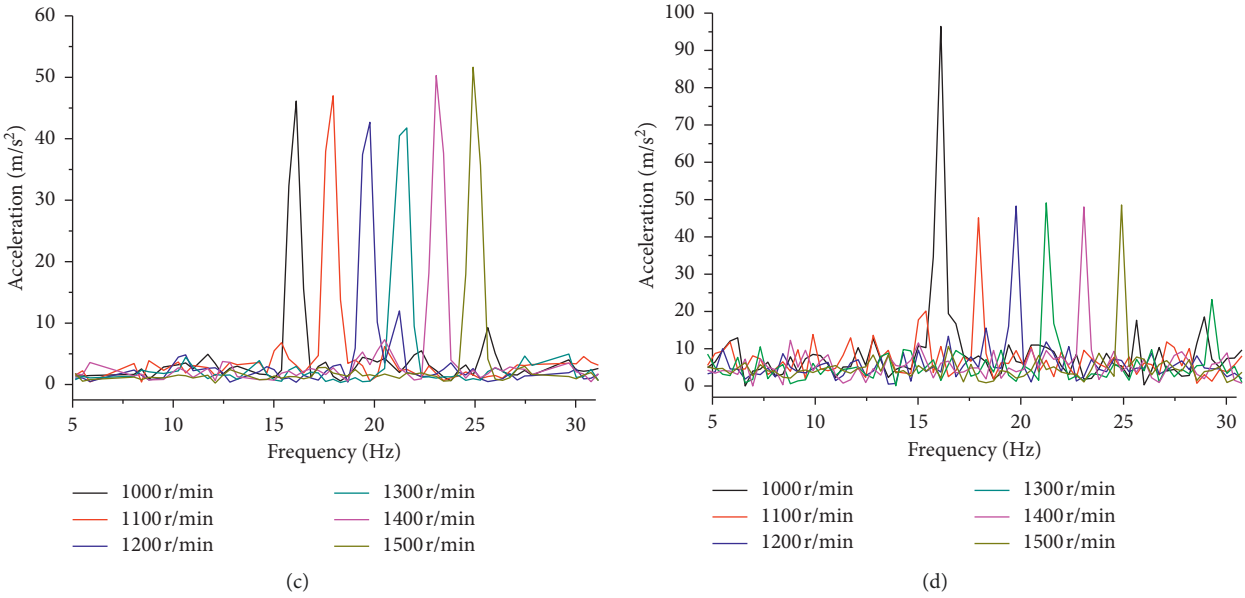

Figure 13: Vibration acceleration near rotation frequency of the JW6314 three-phase motor. (a) Sensor 1 on the base. (b) Sensor 2 on the cylinder. (c) Sensor 3 on the base. (d) Sensor 4 on the cylinder.

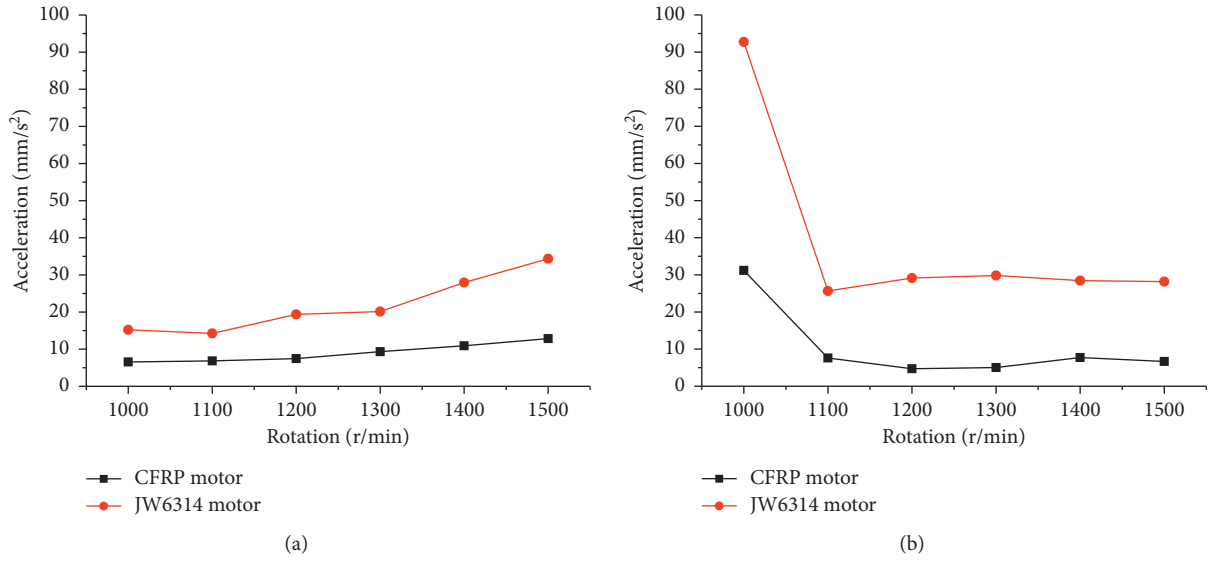

Figure 14: Continued.

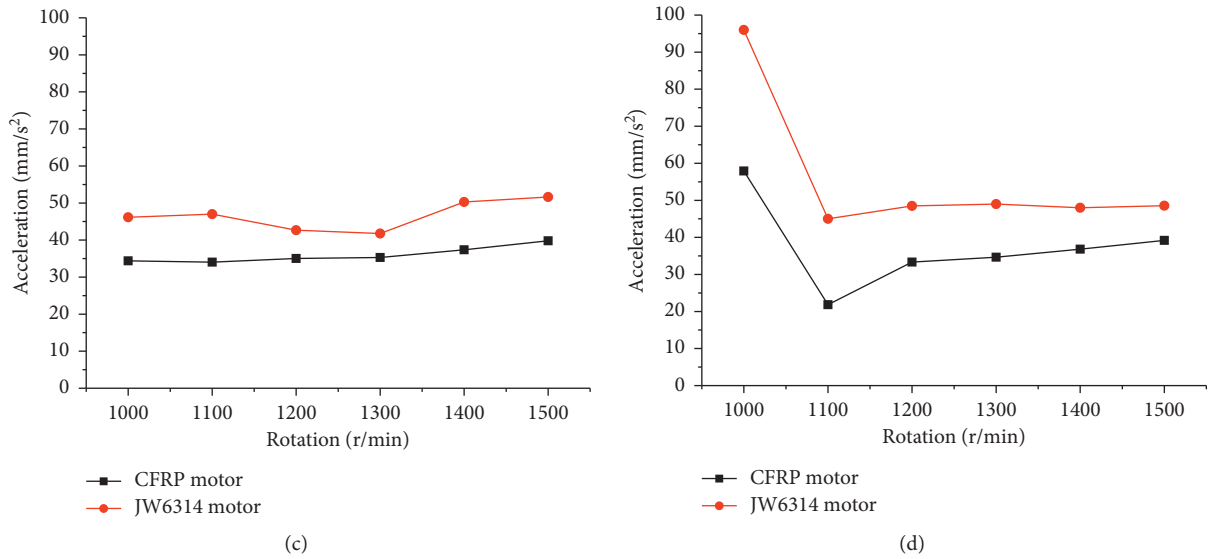

Figure 14: Comparison of acceleration amplitude of two kinds of motors. (a) Sensor 1 on the base. (b) Sensor 2 on the cylinder. (c) Sensor 3 on the cylinder. (d) Sensor 4 on the cylinder.

Table 5: Reduction rate of vibration acceleration of the CFRP frame motor.

Rotating speed (r/min)	Reduction of vibration acceleration			
	Sensor 1 on the base (%)	Sensor 2 on the cylinder (%)	Sensor 3 on the cylinder (%)	Sensor 4 on the cylinder (%)
1000	132	197	34	66
1100	108	237	38	107
1200	159	519	22	45
1300	115	493	18	42
1400	156	268	35	30
1500	168	322	30	24

reduction. With the increase of motor speed, the vibration acceleration of the CFRP motor bases and cylinder shells in the vertical direction (sensor 1 and 3) shows a general trend of growth, while the vibration acceleration of the cylinder shells in the horizontal direction (sensor 2 and 4) suddenly decreases to the minimum value at 1100 r/min and then remains unchanged. It can be seen that the change trend of Figures 14(b) and 14(d) is the same, but the amplitudes are different. Sensor 2 and 4 are lying in the same plane theoretically, but there is an error when arranging the sensor.

The vibration acceleration on the base and cylinder shell of the CFRP motor compared with the JW6314 motor is shown in Table 5. It can be seen that the vibration acceleration on the base of the CFRP motor was reduced more than twice near the rotational frequency of the motor and the vibration acceleration was reduced, and the minimum is 18% and maximum is 519% on the cylindrical shell. Overall, the CFRP motor frame has better vibration amplitude reduction than the aluminum alloy frame motor.

6. Conclusion

In this paper, a CFRP motor frame is designed and the natural frequency and damping are studied. The damping ratio model of the CFRP motor frame is established based on the strain energy method and verified by experiments. The vibration amplitude reduction during its operation is compared with the metal frame motor. The following conclusions can be drawn:

(1) The CFRP motor frame has the same first three-mode vibration shape as aluminum alloy frame, but the natural frequency of the CFRP frame is about 9 times of the aluminum alloy frame

(2) The errors between the numerical calculation of the damping ratio of the CFRP motor frame and the experimental results are less than 15%, indicating that the established modal strain energy model is accurate

(3) Comparing the vibration acceleration of the CFRP motor and JW6314 motor at different speeds in

frequency domain, the results show that the maximum vibration amplitude reduction on the cylindrical shell of the CFRP motor frame is 519%, which proves that the CFRP motor frame can reduce vibration amplitude more than the aluminum alloy motor frame

Data Availability

The data used to support the findings of this study are available from the corresponding author upon request.

Conflicts of Interest

The authors declare that there are no conflicts of interest regarding the publication of this paper.

Acknowledgments

This project was supported by the National Natural Science Foundation of China (Grant No. 51975435).

References

[1] W. Mendon, E. Medeiros, A. Pereira et al., "The dynamic analysis of rotors mounted on composite shafts with internal damping," *Composite Structures*, vol. 167, no. 1, pp. 50–62, 2017.

[2] F. Druesne, J. Hallal, and V. P. Lanfranchi, "Modal stability procedure applied to variability in vibration from electromagnetic origin for an electric motor," *Finite Elements in Analysis and Design*, vol. 122, no. 1, pp. 61–74, 2016.

[3] H. Lin, Y. Y. Xiang, and Y. Yang, "Coupled vibration analysis of CFRP cable-tube system under parametric excitation in submerged floating tunnel," *Procedia Engineering*, vol. 166, no. 5, pp. 45–52, 2016.

[4] M. Khazaei Poul, F. Nateghi-Alahi, and X. L. Zhao, "Experimental testing on CFRP strengthened thin steel plates under shear loading," *Thin-Walled Structures*, vol. 109, no. 1, pp. 217–226, 2016.

[5] R. Capozucca and B. Bonci, "Notched CFRP laminates under vibration," *Composite Structures*, vol. 122, no. 3, pp. 367–375, 2015.

[6] R. D. Adams and D. G. C. Bacon, "Measurement of the flexural damping capacity and dynamic Young's modulus of metals and reinforced plastics," *Journal of Physics D: Applied Physics*, vol. 6, no. 1, pp. 27–41, 1973.

[7] R. G. Ni and R. D. Adams, "A rational method for obtaining the dynamic mechanical properties of laminae for predicting the stiffness and damping of laminated plates and beams," *Composites*, vol. 15, no. 3, pp. 193–199, 1984.

[8] E. K. Billups and M. N. Cavalli, "2D damping predictions of fiber composite plates: layup effects," *Composites Science and Technology*, vol. 68, no. 3-4, pp. 727–733, 2008.

[9] A. Martone, M. V. Antonucci, and M. Giordano, "A simplified approach to model damping behaviour of interleaved carbon fibre laminates," *Composites Part B: Engineering*, vol. 97, no. 1, pp. 103–110, 2016.

[10] M. Assarar, W. Zouari, R. Ayad, H. Kebir, and J.-M. Berthelot, "Improving the damping properties of carbon fibre reinforced composites by interleaving flax and viscoelastic layers," *Composites Part B: Engineering*, vol. 152, no. 3, pp. 248–255, 2018.

[11] H. Abramovich, A. D. Govich, and A. Grunwald, "Damping measurements of laminated composite materials and aluminum using the hysteresis loop method," *Progress in Aerospace Sciences*, vol. 78, no. 1, pp. 8–18, 2015.

[12] M. R. Maheri, "The effect of layup and boundary conditions on the modal damping of FRP composite panels," *Journal of Composite Materials*, vol. 45, no. 13, pp. 1411–1422, 2011.

[13] M. Rueppel, J. Rion, C. Dransfeld, C. Fischer, and K Masania, "Damping of carbon fibre and flax fibre angle-ply composite laminates," *Composites Science and Technology*, vol. 146, no. 2, pp. 1–9, 2017.

[14] Y. Hong, X. D. He, and R. G. Wang, "Vibration and damping analysis of a composite blade," *Materials & Design*, vol. 34, no. 1, pp. 98–105, 2012.

[15] J. Zhang, H. Yang, C. Chen, and Z. Zhang, "Structure and modal analysis of carbon fiber reinforced polymer raft frame," *Journal of Low Frequency Noise, Vibration and Active Control*, vol. 37, no. 3, pp. 577–589, 2018.

[16] X. Wen, W. Li, Y. Fang, C. Song, and J. Zhang, "Design and vibration isolation performance of truss-type CFRP raft frame," *Shock and Vibration*, vol. 2019, pp. 1–10, 2019.

[17] R. D. Adams and D. G. C. Bacon, "Effect of fibre orientation and laminate geometry on the dynamic properties of CFRP," *Journal of Composite Materials*, vol. 7, no. 4, pp. 402–428, 1973.

[18] M. Yang, Y. Hu, J. Zhang, G. Ding, and C. Song, "Analytical model for flexural damping responses of CFRP cantilever beams in the low-frequency vibration," *Journal of Low Frequency Noise, Vibration and Active Control*, vol. 37, no. 4, pp. 669–681, 2018.